Physics Letters B 287 (1992) 191–202
North-Holland

PHYSICS LETTERS B

Rare decays $B \to X_d + \gamma$ in the standard model

A. Ali
Deutsches Elektronen Synchrotron DESY, W-2000 Hamburg, FRG

and

C. Greub [1]
Universität Zürich, CH-8001 Zurich, Switzerland

Received 3 April 1992; revised manuscript received 26 May 1992

We present an estimate of the inclusive decay rate and photon energy- and hadron mass-spectrum for the CKM-suppressed radiative rare decays $B \to X_d + \gamma$, based on perturbative QCD and a phenomenological model for the B-meson wave function (here X_d denotes nonstrange hadrons). Present constraints on $|V_{td}|$ are used to predict $BR(B \to X_d + \gamma) = (0.8\text{–}4) \times 10^{-5}$ for the top quark mass in the range $100 \leqslant m_t \leqslant 200$ GeV. From the inclusive invariant hadron-mass spectrum and using vector meson dominance in the region $m(X_d) \leqslant 1$ GeV, we estimate the branching ratio for the exclusive rare decay mode $B \to \rho + \gamma$ and the ratio $\Gamma(B \to \rho + \gamma)/\Gamma(B \to K^* + \gamma)$. The importance of measuring these decays in determining the CKM matrix element $|V_{td}|$ is emphasized.

1. Introduction

Flavour changing neutral current (FCNC) processes in the standard model (SM) are governed by one-loop graphs (penguins and boxes). They provide valuable information on the properties of the top quark, in particular its mass and the three CKM matrix elements (V_i; $i = d, s, b$). The dominant FCNC B-decays involve the transitions $b \to s + X$, where $X = g, \gamma, (\ell^+\ell^-)$, and $\nu\bar{\nu}$. A measurement of their decay rates would determine the CKM matrix element $|V_{ts}|$. These transitions have received quite a bit of theoretical attention [1]. However, one also expects in the SM the FCNC transitions $b \to d + X$. They would manifest themselves through final states such as $B \to \rho + \gamma$, $B \to (\pi, \rho) + \ell^+\ell^-$, and $B \to (\pi, \rho) + \nu\bar{\nu}$. The short distance contributions to these decays depend on the CKM matrix element v_{td}, and hence one anticipates that they are suppressed as compared to the analogous $b \to s + X$ decays. From a theoretical point of view, however, the CKM-suppressed FCNC decays are very interesting, since their measurement would determine the critical matrix element V_{td}, which at present is only loosely constrained due to the unknown top quark mass and imprecise knowledge of the various coupling constants. In this context we emphasize that the relative decay rates $\Gamma(b \to d + X)/\Gamma(b \to s + X)$ are largely free of the hadronic matrix element ambiguities and the unknown top quark mass. We illustrate and quantify this by working out the case of the radiative rare B-decays $B \to X_d + \gamma$ in the SM, using the theoretical framework developed for the $B \to X_s + \gamma$ decays [2,3]. In particular, we present estimates of the branching ratio for the inclusive decay $B \to X_d + \gamma$ and give a profile of the photon-energy and the invariant-hadron-mass distributions. Moreover, using the (plausible) assumption that the invariant mass distributions up to 1 GeV are saturated by the K* (for $B \to X_s + \gamma$) and ρ (for $B \to X_s + \gamma$) resonances, we estimate the branching ratios $BR(B \to K^* + \gamma)$ and $BR(B \to \rho + \gamma)$.

[1] Partially supported by Schweizerischer Nationalfonds.

2. Effective hamiltonian for the decays $B\to X_s+\gamma$ and $B\to X_d+\gamma$

The framework that we use here is that of an effective theory with five quarks, obtained by integrating out the heavier degrees of freedom (top quark and $W^{\pm}$ bosons). In the effective theory one keeps only the operators with the lowest (mass) dimensions since the higher dimension operators are power suppressed by terms of $O(m_b/m_t)$ and $O(m_b/m_W)$. To leading order in the small (weak)-mixing angles, a complete set of dimension-six operators relevant for the processes $b\to s+\gamma$ and $b\to s+\gamma+g$ is contained in the effective hamiltonian

$$H_{\rm eff}(b\to s\gamma)=-\frac{4G_F}{\sqrt{2}}\lambda_t\sum_{j=1}^{8}C_j(\mu)\hat{O}_j(\mu)\,, \tag{1}$$

where G_F is the Fermi coupling constant, $C_j(\mu)$ are the Wilson coefficients evaluated at the scale μ, and $\lambda_t=V_{tb}V_{ts}^*$, with V_{ij} being the Cabibbo–Kobayashi–Maskawa (CKM) matrix elements. The definitions of the various operators, matching conditions $C_i(m_W)$, and the leading log perturbative QCD corrections giving $C_i(\mu)$ with $\mu\ll m_W$ can be seen in ref. [1]. We recall here that $\hat{O}_1$ and $\hat{O}_2$ represent the colour-singlet and colour-octet four-fermion operators, respectively, obtained from the SM charged current lagrangian written in the charge retention form. It is known that the operators $\hat{O}_3$, ..., $\hat{O}_6$, which are the four-fermion operators obtained from the penguin diagrams, enter indirectly in $b\to s+\gamma$ decays due to operator mixing; as their coefficients are small [1], their effect can be neglected. $\hat{O}_7$ and $\hat{O}_8$ are the QED and QCD magnetic moment operators, respectively. It is known from earlier studies that the dominant contribution to $b\to s+\gamma$ and $b\to s+g+\gamma$ are due to the operators $\hat{O}_2$ and $\hat{O}_7$ which are defined as

$$\hat{O}_2=(\bar{c}_{L\alpha}\gamma^{\mu}b_{L\alpha})(\bar{s}_{L\beta}\gamma_{\mu}c_{L\beta}),\quad \hat{O}_7=(e/16\pi^2)\bar{s}_{\alpha}\sigma^{\mu\nu}(m_bR+m_sL)b_{\alpha}F_{\mu\nu}\,,$$
$$L=\tfrac{1}{2}(1-\gamma_5),\quad R=\tfrac{1}{2}(1+\gamma_5)\,. \tag{2}$$

Here e denotes the QED coupling constant. The coefficients $C_2(m_b)$, $C_7(m_b)$, obtained in the leading logarithm approximation [1], and the corresponding coefficients at the scale m_W are listed below:

$$C_2(m_b)=\tfrac{1}{2}(\eta^{-6/23}+\eta^{12/23})C_2(m_W)\,,$$
$$C_7(m_b)=\eta^{-16/23}[C_7(m_W)-\tfrac{58}{135}(\eta^{10/23}-1)C_2(m_W)-\tfrac{29}{189}(\eta^{28/23}-1)C_2(m_W)]\,,$$
$$C_2(m_W)=1,\quad C_7(m_W)=F_2(x)\,, \tag{3}$$

with $\eta=\alpha_s(m_b)/\alpha_s(m_W)$ being the ratio of the QCD coupling constants and $x=m_t^2/m_W^2$. The Inami–Lim function $F_2(x)$ derived from the penguin diagrams is given by [4]

$$F_2(x)=\frac{x}{24(x-1)^4}[6x(3x-2)\log x-(x-1)(8x^2+5x-7)]\,. \tag{4}$$

In writing the expression for $F_2(x)$ we have neglected terms of order $(m_c/m_W)^2$ and $(m_u/m_W)^2$.

We now discuss the modification that has to be implemented for the rare decays $b\to d+\gamma$ and $b\to d+\gamma+g$. To that end we first define the CKM matrix in the Wolfenstein parametrization [5]:

$$V_{\rm CKM\text{-}W}=\begin{pmatrix}1-\frac{1}{2}\lambda^2 & \lambda & A\lambda^3(\rho-i\eta)\\ -\lambda & 1-\frac{1}{2}\lambda^2 & A\lambda^2\\ A\lambda^3(1-\rho-i\eta) & -A\lambda^2 & 1\end{pmatrix}. \tag{5}$$

The representation, $V_{\rm CKM\text{-}W}$, has three real parameters A, λ, and ρ, and a phase η. We recall here that for the decays $b\to s+\gamma(+g)$ the effective hamiltonian was written in the approximation where the CKM factor $\lambda_u=0$, which is reasonable since $\lambda_u\ll\lambda_c,\lambda_t$ ($\lambda_i\equiv V_{ib}V_{is}^*$). For the decays $b\to d+\gamma$ and $b\to d+\gamma+g$ the CKM factors λ_i are replaced by $\xi_i\equiv V_{ib}V_{id}^*$. Now ξ_u, ξ_c and ξ_t are all of the same order of magnitude ($A\lambda^3$) and therefore the corresponding approximation $\xi_u=0$ cannot be made any longer. The differences due to the inclusion of ξ_u to

describe the decays b→d+γ and b→d+g+γ can be most easily built in the effective hamiltonian framework by modifying the operators $\hat{O}_1$ and $\hat{O}_2$, encountered in the decay b→s+γ. The dimension-six operator basis again reads

$$H_{\rm eff}({\rm b}\to{\rm d}\gamma) = -\frac{4G_{\rm F}}{\sqrt{2}}\,\xi_{\rm t}\sum_{j=1}^{8} C_j(\mu)O_j(\mu)\,. \tag{6}$$

The operators O_1 and O_2 are defined as

$$O_1 = -\frac{\xi_{\rm c}}{\xi_{\rm t}}\,(\bar{c}_{{\rm L}\beta}\gamma^{\mu}b_{{\rm L}\alpha})(\bar{d}_{{\rm L}\alpha}\gamma_{\mu}c_{{\rm L}\beta}) - \frac{\xi_{\rm u}}{\xi_{\rm t}}\,(\bar{u}_{{\rm L}\beta}\gamma^{\mu}b_{{\rm L}\alpha})(\bar{d}_{{\rm L}\alpha}\gamma_{\mu}u_{{\rm L}\beta})\,,$$

$$O_2 = -\frac{\xi_{\rm c}}{\xi_{\rm t}}\,(\bar{c}_{{\rm L}\alpha}\gamma^{\mu}b_{{\rm L}\alpha})(\bar{d}_{{\rm L}\beta}\gamma_{\mu}c_{{\rm L}\beta}) - \frac{\xi_{\rm u}}{\xi_{\rm t}}\,(\bar{u}_{{\rm L}\alpha}\gamma^{\mu}b_{{\rm L}\alpha})(\bar{d}_{{\rm L}\beta}\gamma_{\mu}u_{{\rm L}\beta})\,. \tag{7}$$

With the operators defined in this basis, the matching conditions, $C_i(m_{\rm W})$, and the corresponding Wilson coefficients at the scale $\mu = m_{\rm b}$, $C_i(m_{\rm b})$, are precisely the same for the decays b→d+γ as given above for the b→s+γ case.

3. The decays b→d+γ and b→s+γ

We start with the lowest order (one-loop) results for the decay rates b→(s, d)+γ. The only contribution to these two-body decays is due to the operator O_7. A straightforward calculation yields

$$\Gamma({\rm b}\to{\rm s}+\gamma) = |\lambda_{\rm t}|^2\,\frac{G_{\rm F}^2 m_{\rm b}^5\alpha}{32\pi^4}\,|F_2(x)|^2\,, \tag{8}$$

$$\Gamma({\rm b}\to{\rm d}+\gamma) = |\xi_{\rm t}|^2\,\frac{G_{\rm F}^2 m_{\rm b}^5\alpha}{32\pi^4}\,|F_2(x)|^2\,, \tag{9}$$

where we have dropped terms of $O(m_{\rm s}/m_{\rm b})$ and $O(m_{\rm d}/m_{\rm b})$. The respective rates for radiative rare B-decays may be expressed in terms of the branching ratio for the inclusive CC semileptonic B-decays B→$(X_{\rm c}, X_{\rm u})\ell\nu_\ell$, which has been well measured. This would remove their annoying $m_{\rm b}^5$-dependence. Deferring the numerical estimates for the branching ratios for the time being, we note the following relation between the SM decay rates [6]:

$$\frac{{\rm BR}({\rm b}\to{\rm d}+\gamma)}{{\rm BR}({\rm b}\to{\rm s}+\gamma)} = \frac{|V_{\rm td}|^2}{|V_{\rm ts}|^2} \tag{10}$$

The relation in eq. (10) is representative of a number of FCNC B-decays involving the CKM-allowed b→s+X and CKM-suppressed b→d+X transitions in the standard model. In our opinion, checking this and similar relations experimentally is extremely important both for the unitarity of the CKM matrix, as well as determination of the matrix element $V_{\rm td}$. We shall estimate the ratio in eq. (10) later, making use of the available constraints on the CKM matrix elements. However, as an order of magnitude, we expect it to be $O(\lambda^2) \simeq 0.05$.

In what follows, we study the modification of this relation due to QCD corrections. There are two kinds of corrections that one has to incorporate: First, there is the QCD-renormalization of the Wilson coefficients of the relevant operators, discussed above. For the two-body decays b→s+γ and b→d+γ, only the magnetic moment operator O_7 contributes and hence the QCD corrected rates can be represented by formulae similar to the ones given above for the lowest order, with the function $F_2(x)$ replaced by the QCD corrected function $C_7(m_{\rm b})$. Since this scaling is identical in the two-body decays b→s+γ and b→d+γ, the ratio (10) is not renormalized by the QCD scaling of the Wilson coefficients. Second, one has to take into account gluon bremsstrahlung correc-

tions, $b\to(s, d)+\gamma+g$ to get non-trivial photon energy spectra. These corrections, of course, also modify the rates for the inclusive decays $B\to X_d+\gamma$ and $B\to X_s+\gamma$. Neglecting the small contributions of the operators O_3, ..., O_6, the gluon bremsstrahlung corrections involve the operators O_1, O_2, O_7, and O_8. Note that the operators O_1 and O_2 cause a non-trivial dependence on the CKM matrix elements. It leads to non-factorizing corrections (in the CKM parameters) to the inclusive decay width $\Gamma(B\to X_d+\gamma)$. We estimate theses corrections in the next sections.

4. QCD bremsstrahlung corrections to $b\to(s, d)+\gamma$

In specifying the operator basis and carrying out the calculations for the decays $b\to d+\gamma$ and $b\to d+g+\gamma$, we shall remain as close as possible to the well-studied decays $b\to s+\gamma$ and $b\to s+g+\gamma$, reported by us in ref. [2,3]. In the approximation of keeping only the contributions of the operators O_1, O_2, O_7, and O_8, the amplitude for the processes $b\to d+\gamma+g$ can be calculated from the diagrams shown in fig. 1. The $O(\alpha\alpha_s)$ calculations for $b\to s+\gamma+g$ were done in refs. [2,3], where dimensional regularization (and Landau gauge) were used, which we also employ here for the $b\to d+\gamma+g$ case. In the diagrams associated with O_1 and O_2 both u- and c-quarks propagate in the loop. Again, the diagrams associated with O_1 vanish due to the colour structure. Also, the coefficient of the operator O_8 gets suppressed after including QCD effects and its contribution is neglected. In the following we therefore only keep the contributions associated with O_2 and O_7. Note, that the diagrams where only one boson (gluon or photon) is radiated from an internal quark line vanish in dimensional regularization and hence are not shown.

Concerning the photon energy spectra in the decays $b\to(s, d)+\gamma+g$, it is to be noted that they have a nonintegrable infrared singularity for $E_g\to 0$, showing up as $E_\gamma\to E_\gamma^{\max}$. Adding the contributions of the processes $b\to(s, d)+\gamma+g$ with their respective virtual QCD corrections, the singularity cancels in a distribution sense [2,3]. The end-point spectra, however, show sensitivity to the leftover effects of the (cancelled) infrared singularity,

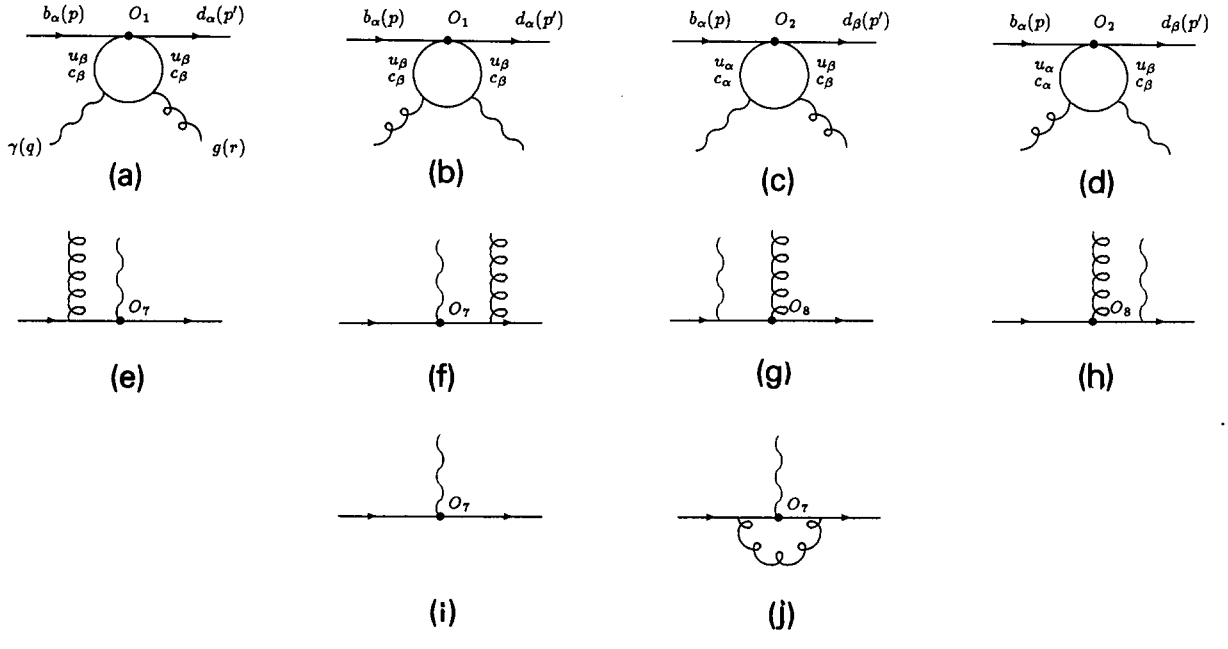

Fig. 1. Feynman diagrams contributing to the decays $b\to d+\gamma$ and $b\to d+g+\gamma$.

with the photon-energy distribution $d\Gamma/dx_\gamma$ rising very steeply near the end-point, $x_\gamma \simeq 1$ (here x_γ is the fractional energy of the photon, $x_\gamma = E_\gamma/E_\gamma^{\max}$). To remedy this, one often resorts to (an all-order) resummation of the leading (infrared) logarithms. The resummed theory provides a more reliable description of the spectra near the end-point. In refs. [2,3], the leading terms (in $O(\alpha_s)$) were isolated analytically and exponentiated for the decays $b\to s+\gamma+(g)$ in the region $x_\gamma \to 1$. We discuss exponentiation procedures for the end-point photon energy spectrum in the decays $b\to d+\gamma(+g)$ here.

We find it convenient to express the photon energy spectrum as a sum of the following parts:

$$\frac{d\Gamma}{dx_\gamma} = \frac{d\Gamma_F}{dx_\gamma} + \frac{d\Gamma_7}{dx_\gamma}. \tag{11}$$

The first term on the RHS of eq. (11) is free of infrared singularities. It contains the square of the matrix element of the operator O_2 and the interference term of O_2 and O_7; it can be written as a one-dimensional integral over the gluon energy in the process $b\to d+g+\gamma$ [2,3]:

$$\frac{d\Gamma_F}{dx_\gamma} = \frac{G_F^2 |\xi_t|^2 \alpha\alpha_s (1-r)}{1536\pi^5} \int_{E_g^-}^{E_g^+} (\tau_{22}+\tau_{27})\, dE_g,$$

$$\tau_{22} = \tfrac{8}{9} C_2^2(\mu)(qq')^2 |\tilde\kappa|^2 [(m_b^2 - m_d^2)^2 - 2(m_d^2+m_b^2)(qq')],$$

$$\tau_{27} = \tfrac{64}{3} C_2(\mu) C_7(\mu)(qq')^2 \,\mathrm{Re}(\tilde\kappa)\left(\frac{m_d^2 m_b^2 (qq')}{(pq')(p'q')} - (m_d^2+m_b^2)\right),$$

$$\tilde\kappa = -\frac{\xi_c}{\xi_t}\kappa - \frac{\xi_u}{\xi_t}\frac{4}{qq'}. \tag{12}$$

The limits of the E_g-integration are

$$E_g^- = \tfrac{1}{2} m_b (1-r)(1-x_\gamma), \quad E_g^+ = \tfrac{1}{2} m_b \frac{(1-r)(1-x_\gamma)}{1-x_\gamma(1-r)}, \quad r = (m_d/m_b)^2, \tag{13}$$

and q, q', p and p' denote the four-momenta of the photon, gluon, b-quark and d-quark, respectively. The function κ is defined as

$$\kappa = \frac{4[2G(t)+t]}{(qq')t},$$

where $t = 2(qq')/m_c^2$ and $G(t)$ is defined by the integral

$$G(t) = \int_0^1 \frac{dy}{y} \log[1 - ty(1-y) - i\epsilon], \tag{14}$$

which yields

$$G(t) = -2\arctan^2\left(\sqrt{\frac{t}{4-t}}\right), \quad t<4,$$

$$G(t) = -\tfrac{1}{2}\pi^2 + 2\log^2[\tfrac{1}{2}(\sqrt{t}+\sqrt{t-4})] - 2i\pi \log[\tfrac{1}{2}(\sqrt{t}+\sqrt{t-4})], \quad t>4. \tag{15}$$

The $d\Gamma_7$ contribution is identical (up to the replacement $m_s \to m_d$) as in the $b\to s+\gamma+(g)$ case. It has a part due to the exchange of a virtual gluon and a part due to gluon bremsstrahlung. These parts were separately discussed in refs. [2,3]. We give here the expression for

$$\Gamma_7(s_0)=\int_{s_0}^{1}\frac{\mathrm{d}\Gamma_7}{\mathrm{d}x_\gamma}\,\mathrm{d}x_\gamma\,. \tag{16}$$

Doing the indicated x_γ-integration, one gets

$$\Gamma_7(s_0)=V\left(1+\frac{\alpha_s}{3\pi}\Omega\right)\Theta(1-s_0),\quad V=(1-r)^3(1+r)\,\frac{m_b^5}{32\pi^4}\,\alpha G_F^2\,|\xi_t|^2 C_7^2\,. \tag{17}$$

To exponentiate the end-point spectrum, we now split Ω into two contributions: $\Omega=\Omega_1+\Omega_2$ (with $\eta_0\equiv 1-(1-r)s_0$).

$$\Omega_1=\frac{1+r}{1-r}\,[2\log^2\eta_0-4\log\eta_0\log(1-s_0)]+\frac{4}{1-r}\log\eta_0-8\log(1-s_0)+\frac{11r-3}{(1-r)^3}\log\eta_0\,, \tag{18}$$

$$\begin{aligned}\Omega_2=&-4s_0-8\log(1-r)+4\frac{1+r}{1-r}\left[\log(1-r)\log\left(\frac{r}{\eta_0}\right)-\tfrac{1}{3}\pi^2+\mathrm{Li}\left(\frac{r}{\eta_0}\right)+\mathrm{Li}(r)\right]\\&+\frac{1}{(1-r)^3}\left((3r^2-21r+6)(\eta_0-r)+(1+3r)(\eta_0^2-r^2)-\tfrac{2}{3}(\eta_0^3-r^3)-\frac{(1-r^2)(1-s_0)}{\eta_0}\right.\\&\left.-2(1-r)(2-r)(\eta_0\log\eta_0-r\log r)+(1-r)(\eta_0^2\log\eta_0-r^2\log r)-r(13r^2-23r+18)\log r\right).\end{aligned} \tag{19}$$

Ω_2 is finite for $s_0\to 1$ both for $r=0$ and $r\neq 0$. In Ω_1, for $r\neq 0$ only the terms proportional to $\log(1-s_0)$ are singular as $s_0\to 1$. We recall here that in the decay $b\to s+\gamma+g$, we had tacitly assumed that $m_s\neq 0$. There only the terms proportional to $\log(1-s_0)$ in Ω_1 were exponentiated [2,3]. However, in the limit $r\to 0$ (which is more appropriate for the case $b\to d+\gamma$ and $b\to d+\gamma+g$), the variable η_0 becomes $1-s_0$ and therefore also $\log\eta_0$ terms get singular, giving rise to a double log singularity. This is the essential difference in the limiting behaviour for the $r=0$ and $r\neq 0$ cases. In order to guarantee a smooth transition from the $r\neq 0$ to the $r=0$ case, we exponentiate the entire Ω_1 contribution, giving

$$\Gamma_7^{\exp}(s_0)=V\left(1+\frac{\alpha_s}{3\pi}\Omega_2\right)\exp\left(\frac{\alpha_s}{3\pi}\Omega_1\right)\Theta(1-s_0)\,. \tag{20}$$

The exponentiated version of the O_7 contribution to the photon energy spectrum then yields

$$\frac{\mathrm{d}\Gamma_7^{\exp}}{\mathrm{d}x_\gamma}(x_\gamma)=-\left.\frac{\mathrm{d}\Gamma_7^{\exp}(s_0)}{\mathrm{d}s_0}\right|_{s_0\to x_\gamma}, \tag{21}$$

$$\frac{\mathrm{d}\Gamma_7^{\exp}}{\mathrm{d}x_\gamma}=-V\frac{\alpha_s}{3\pi}\exp\left(\frac{\alpha_s}{3\pi}\Omega_1\right)\left[\Omega_2'+\Omega_1'\left(1+\frac{\alpha_s}{3\pi}\Omega_2\right)\right], \tag{22}$$

$$\Omega_1'=-\frac{4}{\eta_0}+\frac{8}{1-s_0}+\frac{3-11r}{\eta_0(1-r)^2}+4\frac{1+r}{1-r}\left(-\frac{(1-r)\log\eta_0}{\eta_0}+\frac{\log\eta_0}{1-s_0}+\frac{(1-r)\log(1-s_0)}{\eta_0}\right), \tag{23}$$

$$\begin{aligned}\Omega_2'=&-\frac{4(1+r)}{\eta_0}\log(1-s_0)+\frac{4(1+r)}{\eta_0}\log\eta_0-4\\&-\frac{1}{(1-r)^2}\left((6-21r+3r^2)+2\eta_0(1+3r)+\frac{(1-r^2)(1-s_0)-\eta_0(1+r)}{\eta_0^2}\right.\\&\left.-2\eta_0^2-2(2-r)(1-r)(1+\log\eta_0)+\eta_0(1-r)(1+2\log\eta_0)\right).\end{aligned} \tag{24}$$

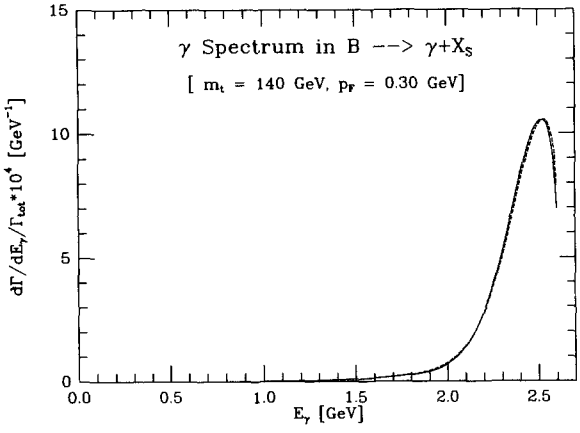

Fig. 2. The influence of two different exponentiation procedures on the final photon energy spectrum is illustrated for $B\to X_s\gamma$, based on eq. (25) (dashed curve) and from refs. [2,3] (solid curve).

Ω_1' and Ω_2' denote the derivatives with respect to s_0 of Ω_1 and Ω_2, which are given in eqs. (18) and (19). Numerically, the two exponentiation procedures lead to small differences in the final γ-spectrum in the $B\to X_s+\gamma$ transitions. These differences are shown in fig. 2 after the incorporation of the wave function effects. As exponentiation is required only near the end-point $x_\gamma\to 1$, we use the exponentiated form in the region $x_\gamma > x_{\rm crit}$ only. For numerical calculations we take $x_{\rm crit}=0.85$. To summarize, eq. (11) is now replaced by

$$\frac{d\Gamma}{dx_\gamma}=\frac{d\Gamma_F}{dx_\gamma}+\Theta(x_{\rm crit}-x_\gamma)\frac{d\Gamma_7}{dx_\gamma}+\Theta(x_\gamma-x_{\rm crit})\frac{d\Gamma_7^{\rm exp}}{dx_\gamma}. \tag{25}$$

The absolute branching ratio for the decays $B\to X_d+\gamma$ depends on m_t and the CKM matrix-element ratio $|V_{td}|^2/|V_{bc}|^2$. Whereas its measurement will provide one of the best determinations of the CKM matrix element $|V_{td}|$, for the time being one could only put a bound on its expected value by constraining $|V_{td}|$ from present data, such as $x_d=(\Delta m)_B/\Gamma$ for the B_d–$\bar{B}_d$ system, the *CP*-violating parameter in the kaon system $|\epsilon|$, and the ratio $|V_{bu}|/|V_{bc}|$. These bounds and numerical estimates are discussed in the next section.

5. Numerical analysis

First, we give an estimate of the inclusive branching ratio $BR(B\to X_d+\gamma)$, which is modelled after the partonic decays $b\to d+\gamma$ and $b\to d+g+\gamma$. Second, we present the shape of the γ-energy spectrum and the related spectrum of the hadronic invariant mass. Third, we extract the branching ratios $BR(B\to\rho+\gamma)$ and $BR(B\to K^*+\gamma)$, as well as the relative rate $BR(B\to\rho+\gamma)/BR(B\to K^*+\gamma)$, using vector meson dominance for the hadronic mass below 1 GeV.

5.1. Estimate of the inclusive branching ratio for $B\to X_d+\gamma$

The branching ratio for the inclusive decay $B\to X_d+\gamma$ is calculated using the relation

$$BR(B\to X_d+\gamma)\equiv\frac{\Gamma(B\to X_d+\gamma)}{\Gamma_{\rm tot}}, \tag{26}$$

where $\Gamma(B\to X_d+\gamma)$ is given in eq. (25) and the b-quark total width, $\Gamma_{\rm tot}$, is obtained from the QCD-improved spectator model:

Table 1
Values of the coefficients D_i entering in eq. (28) as a function of m_t.

m_t (GeV)	D_1	D_2	D_3	D_4
100	0.15	0.21	0.04	0.14
120	0.17	0.20	0.04	0.13
140	0.18	0.18	0.04	0.12
160	0.19	0.17	0.04	0.11
180	0.20	0.17	0.03	0.10
200	0.21	0.16	0.03	0.10

$$\Gamma_{\rm tot}=(r_{\rm u}|V_{\rm ub}|^2+r_{\rm c}|V_{\rm cb}|^2)\Gamma_0,\quad \Gamma_0=\frac{m_{\rm b}^5 G_{\rm F}^2}{192\pi^3},\quad r_{\rm u}\approx 7,\quad r_{\rm c}\approx 3,\quad |V_{\rm cb}|=A\lambda^2,\quad |V_{\rm ub}|/|V_{\rm cb}|\approx 0.1. \tag{27}$$

The values of r_u and r_c include phase space and QCD corrections [7]. The dependence on the b quark mass m_b cancels to a large extent in $BR(B\to X_d+\gamma)$. Due to the contribution of the operator O_2 in $b\to d+g+\gamma$ the dependence of the decay rate on the CKM matrix element does not factorize any longer. This dependence can be written explicitly as

$$BR(B\to X_d+\gamma)=D_1|\xi_t|^2\left(1-\frac{1-\rho}{(1-\rho)^2+\eta^2}D_2-\frac{\eta}{(1-\rho)^2+\eta^2}D_3+\frac{D_4}{(1-\rho)^2+\eta^2}\right), \tag{28}$$

where the coefficients D_i do not depend on the CKM matrix. Their m_t dependence is shown in table 1 (for $m_c=1.68$ GeV, $m_b=5$ GeV, $m_d=0$, $\alpha_s=0.23$, $A=0.926$ and $\lambda=0.220$). The coefficients $D_1,\ldots,D_4$ are not very sensitive to m_t. To get the inclusive branching ratio as a function of m_t, one has to vary the CKM parameters ρ and η over the presently allowed range. For this purpose we use the following experimental inputs:

$$\left|\frac{V_{\rm ub}}{V_{\rm cb}}\right|=0.14\pm 0.05\,, \tag{29}$$

$$|\epsilon|=(2.26\pm 0.02)\times 10^{-3}\,, \tag{30}$$

$$x_{\rm d}=0.67\pm 0.10\,. \tag{31}$$

While the bounds on the ratio $|V_{ub}/V_{cb}|$ give directly $\sqrt{\rho^2+\eta^2}=0.64\pm 0.23$, one has to take into account the m_t-dependence of $|\epsilon|$ and x_d as well as specify other quantities. We use the following expressions for $|\epsilon|$ and x_d [8]:

$$|\epsilon|=\frac{G_{\rm F}^2 f_{\rm K}^2 m_{\rm K} m_{\rm W}^2}{6\sqrt{2}\pi^2\Delta m_{\rm K}}B_{\rm K}(A^2\lambda^6\eta)\{x_{\rm c}[\eta_{\rm ct}f_3(x_{\rm c},x_{\rm t})-\eta_{\rm cc}]+\eta_{\rm tt}x_{\rm t}f_2(x_{\rm t})A^2\lambda^4(1-\rho)\}\,. \tag{32}$$

Here, the η_i are QCD correction factors, $\eta_{cc}\simeq 0.85$, $\eta_{tt}\simeq 0.61$, $\eta_{ct}\simeq 0.36$ for $\Lambda_{\rm QCD}=200$ MeV, [9], $m_K=498$ MeV, $\Delta m_K=3.5\times 10^{-12}$ MeV, $f_K=160$ MeV, $x_i\equiv m_i^2/M_W^2$, and the functions f_2 and f_3 are given by

$$f_2(x)=\tfrac{1}{4}+\frac{9}{4}\frac{1}{(1-x)}-\frac{3}{2}\frac{1}{(1-x)^2}-\frac{3}{2}\frac{x^2\ln x}{(1-x)^3},\quad f_3(x,y)=\ln\frac{y}{x}-\frac{3y}{4(1-y)}\left(1+\frac{y}{1-y}\ln y\right). \tag{33}$$

The final parameter in the expression for $|\epsilon|$ is B_K, which represents our ignorance of the matrix element $\langle K^0|[\bar d\gamma^\mu(1-\gamma_5)s]^2|\bar K^0\rangle$. We shall take $B_K=\frac{2}{3}\pm\frac{1}{6}$. This leads to the two hyperbolae in fig. 3.

We now turn to B_d^0–$\bar B_d^0$ mixing, which is dominated by the t-quark exchange:

$$x_{\rm d}\equiv\frac{(\Delta m)_{\rm B}}{\Gamma}=\tau_{\rm B}\frac{G_{\rm F}^2}{6\pi^2}m_{\rm W}^2 m_{\rm B}(f_{\rm B_d}^2 B_{\rm B_d})\eta_{\rm B}x_{\rm t}f_2(x_{\rm t})|\xi_{\rm t}|^2\,. \tag{34}$$

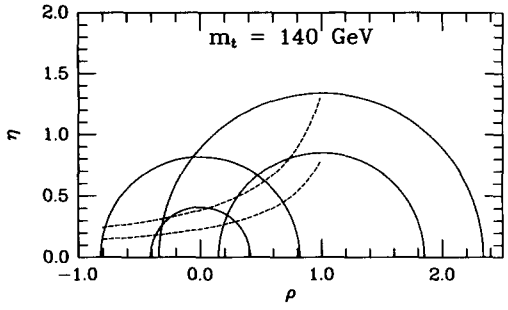

Fig. 3. Constraints on the CKM parameters $(\rho, \eta)$from x_d, $|\epsilon|$ and $|V_{ub}|/|V_{cb}|$ measurements.

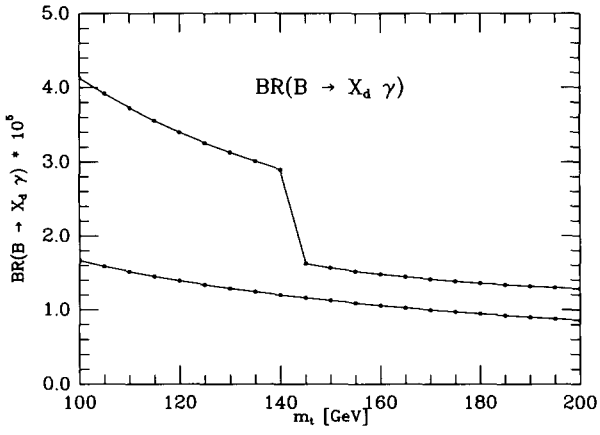

Fig. 4. Upper and lower bounds on the branching ratio $BR(B\to X_d+\gamma)$ as function of m_t, obtained by varying over the allowed range in the (ρ, η) plane, resulting from fig. 3.

Here η_B is the QCD correction factor, for which it was customary to take the leading order result $\eta_B=0.85$ [8]. There now exists a next-to-leading order calculation for η_B, giving an appreciably lower value, $\eta_B=0.55$ [10]. It has been stressed in ref. [11] that other parameters remaining the same, the renormalization of η_B has a significant effect in restricting the allowed (η, ρ) values. In accordance with the recommendations of ref. [11] we set $\eta_B=0.55$, and assume $f_B\sqrt{B_B}=0.20\pm0.03$ GeV, as suggested by recent lattice simulations [12]. In addition, we use $\tau_B=1.28\times10^{-12}$ s, corresponding to the recently updated world average including LEP results, $\tau_B=(1.28\pm0.06)\times10^{-12}$ s [13], and $m_B=5.277$ GeV [14]. The constraint from x_d leads to two semi-circles centered at $(\rho, \eta)=(1,0)$ shown in fig. 3.

The resulting branching ratio $BR(B\to X_d+\gamma)$ is shown in fig. 4 as a function of m_t. With the choice of the parameters, especially the product coupling constant factor $(\eta_B f_{B_d}^2 B_{B_d})$, the constraint from $|\epsilon|$ is irrelevant for $m_t\leqslant 140$ GeV. For $m_t\geqslant 140$ GeV, however, $|\epsilon|$ effectively constrains the upper limit on $|V_{td}|$. This is the reason for the drastic reduction in the uncertainty of $BR(B\to X_d+\gamma)$ for $m_t\geqslant 140$ GeV. From fig. 4 we predict

$$BR(B\to X_d+\gamma)=(0.8\text{–}4)\times10^{-5} \tag{35}$$

for the top quark mass in the range $100\leqslant 200$ GeV. A remark is in order here. The dependence of the branching ratio $BR(B\to X_d+\gamma)$ on the product $(\eta_B f_{B_d}^2 B_{B_d})$ is only indirect; it enters in our analysis since we constrain the CKM parameters η and ρ via x_d. Increasing this factor for a fixed value of m_t decreases $|\xi_t|$ and vice versa. Since $BR(B\to X_d+\gamma)$ also depends on $|\xi_t|^2$, the same behaviour is expected for this branching ratio, though there is a residual dependence of $BR(B\to X_d+\gamma)$ on ρ and η but this is rather mild.

5.2. Photon energy and hadron invariant mass distributions

We now discuss the photon energy spectrum and the invariant mass distribution for $B\to X_d+\gamma$. Our starting point is formula (25), which takes into account the partonic process $b\to d+\gamma$ and $b\to d+g+\gamma$ for the b-quark decaying at rest. This parton level distribution is then folded with a non-perturbative model to take into account the B-meson wave function effects. Since this model has been used extensively in the analysis of B-decays [15,16], and in the present context it has been explained in ref. [3], we shall not elaborate on it any further. We only recall that the (assumed) gaussian distribution of the b-quark momentum $p=|\boldsymbol{p}|$ is characterized by a single parameter, p_F, the average Fermi momentum, which has been experimentally constrained to be $0.21\leqslant p_F\leqslant 0.39$

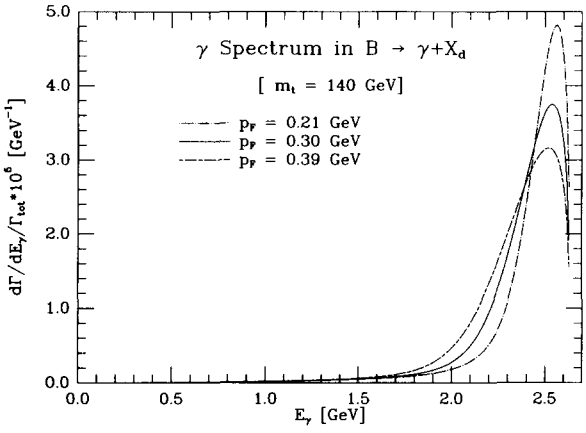

Fig. 5. Photon energy spectrum from the decays $B \to X_d + \gamma$ for $m_t = 140$ GeV and the indicated values of the model parameter p_F. The curve corresponds to the choice $(\rho, \eta) = (0.2, 0.4)$.

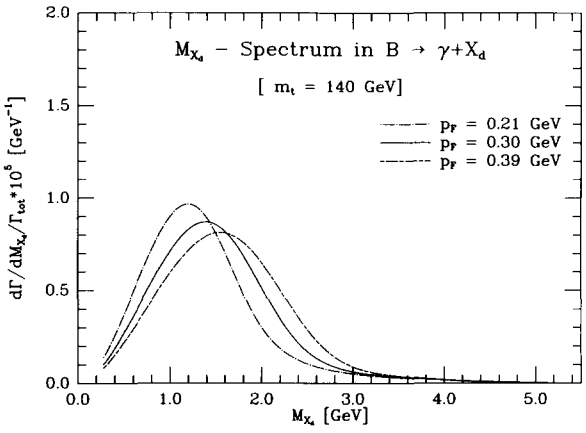

Fig. 6. Hadronic invariant mass distribution in the decay $B \to X_d + \gamma$ for $m_t = 140$ GeV and the indicated values of the model parameter p_F, and with the choice $(\rho, \eta) = (0.2, 0.4)$.

GeV from a recent analysis of the CLEO data [17], with the number from the ARGUS analysis [18] very similar. The resulting photon energy spectrum is shown in fig. 5 for $m_t = 140$ GeV and $(\rho, \eta) = (0.2, 0.4)$, which corresponds to a value in the middle of the allowed (ρ, η) region in fig. 3 and yields $|V_{td}| \simeq 8.8 \times 10^{-3}$. The other parameters are $m_c = 1.68$ GeV, $m_u = m_d = 0$. The spectrum is normalized using Γ_{tot} given in eq. (27), where the parameter m_b has now been traded off in terms of m_B and p_F. A functional relationship for the decays $B \to X_d + \gamma$ is $m_b^2 \simeq m_B^2 - 2 m_B p_F \cdot 1.28$, which reproduces the partonic branching ratio to within a few percent. Finally, fig. 6 shows the hadronic invariant mass distribution in the process $B \to X_d + \gamma$. We note that the invariant mass spectrum for the decays $B \to X_d + \gamma$ and $B \to X_s + \gamma$ are very similar (with obvious threshold difference) and rather broad with peaks around 1.3–1.4 GeV, depending on the model parameters.

5.3. *Estimates for BR(B→ρ+γ) and BR(B→ρ+γ)/BR(B→K*+γ)*

Having the hadronic invariant mass distribution for the decays $B \to X_d + \gamma$ and $B \to X_s + \gamma$, one could attempt to estimate the exclusive branching ratios using the assumption of vector meson dominance in the low-mass part of the invariant hadron mass spectrum. The motivation of doing this comes from experimental studies in semileptonic D-decays, in which the hadronic mass spectrum in the range $m_K + m_\pi \leqslant m_{X_s} \leqslant 1.0$ GeV is found to be completely saturated by the K*-resonance. Although analogous information from the Cabibbo suppressed decays $c \to d \ell \nu_\ell$ and $b \to u \ell \nu_\ell$ is still not at hand, it is reasonable to assume that in the mass range between $2m_\pi$ and 1.0 GeV, the decays $B \to X_d + \gamma$ will be dominated by the ρ-resonance. Following this argument, we integrate the spectrum in the decays $B \to X_d + \gamma$ in the range

$$2m_\pi \leqslant M_{X_d} \leqslant 1 \text{ GeV} \tag{36}$$

to estimate the branching ratio for $B \to \rho + \gamma$. This branching ratio is shown in table 2, where the entries again correspond to the central values in fig. 3, namely $(\rho, \eta) = (0.2, 0.4)$. It turns out that to a precision better than 1% this branching ratio depends on ρ and η only through the combination $|\xi_t|^2 / |V_{bc}|^2 = \lambda^2 [(1-\rho)^2 + \eta^2]$. The reason for this is not too difficult to understand, since in this region the magnetic moment operator O_7 dominates and it only depends on $|\xi_t|$, as can be seen from the effective hamiltonian for $b \to d + \gamma + (g)$. We estimate

$$\mathrm{BR}(B \to \rho + \gamma) = (2 - 4.6) \times 10^{-6} \times \left(\frac{|V_{td}|^2}{7.78 \times 10^{-5}} \right), \tag{37}$$

Table 2
Branching ratio for the decay $B \to \rho + \gamma$ in units of $10^{-6} \times (|V_{td}|^2 / 7.78 \times 10^{-5})$.

p_F (GeV)	m_t (GeV)		
	100	140	200
0.21	3.2	3.8	4.6
0.30	2.4	2.9	3.4
0.39	2.0	2.4	2.8

Table 3
Branching ratio for the decay $B \to K^* + \gamma$ in units of 10^{-5}.

p_F (GeV)	m_t (GeV)		
	100	140	200
0.21	5.4	6.5	7.8
0.30	3.9	4.8	5.7
0.39	3.1	3.8	4.5

taking into account the uncertainties in our model and with m_t in the range $100 < m_t < 200$ GeV. A much firmer prediction is, however, obtained on the relative branching ratios for the decays $B \to \rho + \gamma$ and $B \to K^* + \gamma$:

$$\frac{\Gamma(B \to \rho + \gamma)}{\Gamma(B \to K^* + \gamma)} = (0.062) \times \left(\frac{|V_{td}|^2}{7.78 \times 10^{-5}} \right). \tag{38}$$

The remaining m_t and p_F dependence in this ratio is negligible. To be complete we give in table 3 the numbers for the branching ratio $BR(B \to K^* + \gamma)$ as function of m_t and p_F, by using the same values of the input parameters as in the calculation of $BR(B \to \rho + \gamma)$. With the estimates for the branching ratio $BR(B \to K^* + \gamma) = (3\text{–}8) \times 10^{-5}$ calculated here and in refs. [2,3] and the present experimental bound $BR(B \to K^* + \gamma) < 9.2 \times 10^{-5}$ (90% CL) [19], we feel that the discovery of this channel is just around the corner. It is conceivable that the CKM-suppressed rare decays discussed here, in particular $B \to \rho + \gamma$, can be measured in a first generation B-factory experiment, or perhaps at LEP and CLEO with $O(10^7)$ B-hadrons. This would then provide one of the most reliable estimations of the CKM matrix element $|V_{td}|$.

Acknowledgement

We acknowledge our appreciation to the referee of our manuscript for suggesting the use of the improved QCD calculations for η_B in our numerical analysis.

References

[1] M.A. Shifman, A.I. Vainshtein and V.I. Zakharov, Phys. Rev. D 18 (1978) 2583;
B.A. Campbell and P.J. O'Donnell, Phys. Rev. D 25 (1982) 1989;
S. Bertolini, F. Borzumati and A. Masiero, Phys. Rev. Lett. 59 (1987) 180;
N.G. Deshpande et al., Phys. Rev. Lett. 59 (1987) 183;
R. Grigjanis et al., Phys. Lett. B 213 (1988) 355;
C.S. Lim, T. Morozumi and A.I. Sanda, Phys. Lett. B 218 (1989) 343;
B. Grinstein, M.J. Savage and M.B. Wise, Nucl. Phys. B 319 (1989) 271;
B. Grinstein, R. Springer and M.B. Wise, Nucl. Phys. B 339 (1990) 269;
G. Cella et al., Phys. Lett. B 248 (1990) 181;
M. Misiak, Phys. Lett. B 269 (1991) 161;
A. Ali and T. Mannel, Phys. Lett. B 264 (1991) 447;
A. Ali, T. Mannel and T. Morozumi, Phys. Lett. B 273 (1991) 505.
[2] A. Ali and C. Greub, Z. Phys. C 49 (1991) 431.
[3] A. Ali and C. Greub, Phys. Lett. B 259 (1991) 182.
[4] T. Inami and C.S. Lim, Progr. Theor. Phys. 65 (1981) 297.
[5] L. Wolfenstein, Phys. Rev. Lett. 51 (1983) 1945.

[6] A. Ali, DESY report 91-080 (1991); in: Proc. First Intern A.D. Sakharov Conf. on Physics (Lebedev Institute, Moscow, 1991).
[7] A. Paschos and U. Türke, Phys. Rep. 178 (1989) 145.
[8] A.J. Buras, W. Słominski and H. Steger, Nucl. Phys. B 238 (1984) 529; B 245 (1984) 369.
[9] J. Flynn, Mod. Phys. Lett. A 5 (1990) 877.
[10] A.J. Buras, M. Jamin and P.H. Weisz, Nucl. Phys. B 347 (1990) 491.
[11] A.J. Buras and M.K. Harlander, preprint MPI-PAE/PTh 1/92; TUM-T31-25/92 (1992).
[12] M. Lusignoli et al., Nucl. Phys. B 369 (1992) 139;
C. Alexandrou et al., preprint CERN-TH.6113/91, WUP 91-23, PSI-PR-91-14 (1991).
[13] P. Roudeau, Plenary Session Talk, Joint Intern. Lepton photon Symp. and Europhys. Conf. on High energy physics (Geneva, 1991).
[14] Particle Data group, J.J. Hernández et al., Review of particle properties, Phys. Lett. B 239 (1990) 1.
[15] G. Altarelli et al., Nucl. Phys. B 208 (1982) 365.
[16] A. Ali and E. Pietarinen, Nucl. Phys. B 154 (1979) 519.
[17] CLEO Collab., R. Fulton et al, Phys. Rev. Lett. 64 (1990) 16;
S.Stone, private communication.
[18] ARGUS Collab., H. Albrecht et al., Phys. Lett. B 234 (1990) 409; B 249 (199) 359.
[19] CLEO Collab., M. Battle et al. contrib. paper Joint Intern. Lepton photon Symp. and Europhys. Conf. on High energy physics (Geneva, 1991);
see also M. Danilov, Joint Intern. Lepton photon Symp. and Europhys. Conf. on High energy physics (Geneva, 1991).